JOURNAL OF Applied Polymer SCIENCE

In Situ Silica Reinforcement of Vinyltriethoxysilane-Grafted Styrene–Butadiene Rubber by Sol–Gel Process

Changjie Yin,[1] Qiuyu Zhang,[1] Junwei Gu,[1] Jucheng Zheng,[2] Guangbi Gong,[2] Tao Liang,[2] Hepeng Zhang[1]

[1]Department of Applied Chemistry, School of Science, Northwestern Polytechnical University, Xi'an 710072, China
[2]Petrochemical Research Institute of LAN Zhou Petrochemical Company, LAN Zhou 730060, China
Correspondence to: Q. Zhang (E-mail: qyzhang1803@gmail.com)

ABSTRACT: Grafting polymerization of vinyltriethoxysilane (VTES) onto styrene–butadiene rubber (SBR) was firstly carried out in latex, using potassium persulfate (KPS) as initiator. The grafted SBR was further reinforced with silica produced by sol–gel reaction of tetraethoxysilane (TEOS). The grafted of VTES onto SBR was characterized and confirmed by ATR-FTIR and ^{1}H-NMR. Results revealed that the addition of VTES could considerably improve the content of silica, bound rubber in SBR and utilized efficiency of TEOS. Meanwhile, the curing characteristics and mechanical properties of the vulcanized *in situ* reinforced SBR-*g*-VTES were also investigated and compared with that of the silica-reinforced SBR prepared by mechanical mixing. The delta torque, tensile, and tear strength of *in situ* reinforced SBR-*g*-VTES were higher than that of silica-reinforced SBR. Dynamic mechanical analysis showed that the interaction between silica and SBR of *in situ* reinforced SBR-*g*-VTES was also better than that of the silica-reinforced SBR. © 2012 Wiley Periodicals, Inc. J. Appl. Polym. Sci. 000: 000–000, 2012

KEYWORDS: grafted rubber; tetraethoxysilane; sol–gel method; *in situ* silica

Received 19 January 2012; accepted 23 May 2012; published online
DOI: 10.1002/app.38105

INTRODUCTION

Silica-reinforced styrene–butadiene rubber (SBR) provides several advantages, such as lower rolling resistance and stronger wet skidding resistance, compared with carbon.[1,2] Commonly, silica-reinforced SBR is achieved by mechanical mixing, and silica particles always tend to aggregate.[3–6] In order to solve these problems above, *in situ* synthesis of silica particles within SBR matrixes using sol–gel method of tetraethoxysilane (TEOS) has been developed. The sol–gel method is recognized as a novel method to control the silica particle size and dispersion in rubber.

Among this technique, that of *in situ* silica formation in the rubber matrixes can be operated in solid rubber, rubber solution, and rubber latex. The sol–gel process has been developed and applied to polymers such as butadiene rubber (BR)[7], natural rubbe,[8–11] and SBR[12] and ethylene propylene rubber,[13] as already noted, this method produces fine and well-dispersed silica particles in the rubber matrixes; however, the amount of silica is restricted by the swelling ratio of rubber. Meantime, the sol–gel process also can be performed using rubber solution, where the TEOS and catalyst are directly added into the rubber solution and then it can readily produce the silica/SBR hybrid materials, such as SBR,[14] epoxidized NR,[15] isoprene rubber,[16,17] and carboxylated acrylonitrile–butadiene rubber,[18] as previously mentioned, this method yielded a better reinforcing efficiency than the commercial silica, however, a lot of organic solvent was used during preparation of rubber composites, which is harmful for the environment. The sol–gel process using rubber latex is another method to produce the rubber composites. Yoshikai[19] studied the silica-reinforced raw SBR by sol–gel method of TEOS in latex. They found that the diameter of the dispersed silica particles in cured rubbers could be controlled by the amount of TEOS. However, during this process of preparing reinforced raw rubber, our researches found that a lot of silica particles separated out individually from latex when the reaction products were flocculated by flocculating agents, it is due to the poor interaction between silica and SBR.

Recently, the modification of SBR by grafting with vinyl monomers has gained considerable interest and importance in improving the interaction between rubber and silica.[20] Hashim[9] found that the silica in the final ENR-*g*-APS(epoxidized natural rubber grafted by 3-aminopropyltriethoxysilane) sol–gel vulcanization was chemically bound to the rubber networks. Kawada[21] found that the heat resistance of silane-grafted EPDM was

Table I. Preparation Condition of *In Situ* Reinforced SBR-*g*-VTES Compound

Ingredients	Amounts									
Latex (g)	200.00	200.00	200.00	200.00	200.00	200.00	200.00	200.00	200.00	200.00
VTES (g)	0	0	0	0	0	5	5	5	5	5
TEOS (g)	5	10	20	30	50	5	10	20	30	50

considerably higher than that of native EPDM. Prasassarakich[22] found that the silica was well dispersed within SBR-*g*-MMA(SBR grafted by methyl methacrylate) than native SBR, however, no study has been focused on silane couple agent grafting SBR latex followed by sol–gel process of TEOS. Therefore, it is of great interest to study this topic.

On the basis of our previous works,[23,24] in this study, *in situ* reinforced SBR-*g*-VTES was prepared by in situ TEOS sol–gel process in SBR-*g*-VTES latex. It was anticipated that some silica particles would be chemically bound to the rubber networks, for both VTES and TEOS undergone the same hydrolysis and condensation reactions. The amount of TEOS effecting on the content of silica, bound rubber and utilized efficiency of TEOS for SBR-*g*-VTES were investigated and compared with that of ungrafted SBR. The curing characteristics and mechanical properties of the vulcanized *in situ* reinforced SBR-*g*-VTES and silica-reinforced SBR were also investigated.

EXPERIMENTAL

Materials

The SBR latex (SBRL1500, pH = 8–9, 20.0 wt % solid element, pH = 8.0–9.0, 23.5% styrene content, $ML_{(1+4)}$ of 55.73 at 100°C, M_w = (1.5–4) × 10^5.) was received from LAN Zhou Petroleum Chemical Industrial (LAN Zhou, China). Vinyltriethoxysilane (VTES) and tetraethoxysilane (TEOS) were provided by Shandong Nan duo Silicone (Shandong, China). Potassium persulfate (KPS, CP) was supplied by Shan Pu Chemical (Tianjin, China). Toluene was received from Tianjin Fuyu Chemical (Tianjin, China). The blends of *N*-octyl-*N*-Phenyl-*ρ*-phenylenediamine and 2,2,4-trimethyl-1,2-dihydroquinoline (8PPD), Methyl trialkyl ammonium chloride (AM-2) and the condensation product on dicyandiamide and formaldehyde (TXD), were supplied by LAN Zhou Petroleum Chemical Industrial (LAN Zhou, China). Zinc oxide (ZnO), stearic acid (SA), sulfur (S), *N*-Cyclohexyl-benzothiazyl-sulfenamide (CBS) and Diphenyl-guanigine (DPG) were commercial products. Fumed silica (SiO_2) was supplied by Henan Zhong ya Fine Chemical Engineering (HE NAN, China). Surface areas of silica and carbon were 200 m^2/g.

Preparation of *In Situ* Reinforced SBR-*g*-VTES

The SBR latex was stirred for 30 min in 500-mL flask under N_2 atmosphere, followed by heating to 80°C. The appropriate amount of KPS and VTES were added into the reactor, stirring for 3 h to get the grafted SBR latex (SBR-*g*-VTES latex). Then TEOS of required amount was added. The mixture stood for 3 h at 80°C to promote the sol–gel reaction. Then the reaction products were agglomerated by coagulants (8PPD, AM-2, TXD) after 24 h, washed several times with water, and finally dried under 60°C for 12 h. The preparation conditions were shown in Table I.

Preparation of Vulcanized *In Situ* Reinforced SBR-*g*-VTES and Silica-Reinforced SBR

The curing agents and rubber were mixed with appropriate proportion to get homogeneous blends by two roll mills, and then the mixtures were put into a stainless steel mould and hot pressed at 160°C, 10 MPa to prepare the vulcanized rubber. The recipe of curing agents was shown in Table II.

Characterization

The content of silica and utilized efficiency of TEOS are determined by muffle furnace under 700°C for 6 h. Content of silica (w_1) = m_2/m_1, utilized efficiency of TEOS = Practical content of silica formed by TEOS (w_3)/Theoretical content of silica formed by TEOS (w_2).

$$w_2 = \frac{m_3 \times 60/208}{200 \times 20\% + m_3 \times 60/208} w_4 = \frac{m_4 \times 60/190}{200 \times 20\% + m_4 \times 60/190} w_3 = w_1 - w_4 \times 0.89$$

Where m_1, m_2 are the mass of *in situ* reinforced SBR-*g*-VTES and mass of residue of *in situ* reinforced SBR-*g*-VTES in muffle furnace under 700°C for 6 h, respectively. m_3 and m_4 are the amount of TEOS and VTES, respectively. 60, 190, 208, and 0.89 are the molecular weight of SiO_2, VTES, TEOS, and grafted efficiency of VTES, respectively. Bound rubber was measured as a percentage of insoluble rubber in total rubber for different contents of silica.

The attenuated total teflectance-Fourier transforms infrared reflectance (ATR-FTIR) of SBR and SBR-*g*-VTES was conducted by Fourier transform infrared (Bruker model Tensor 27, German), the *in-situ* reinforced SBR was extracted in an acetone for 24 h to remove the free homopolymer of VTES. ^{1}H-NMR

Table II. Recipe of Curing Agents

Material	Content (g)	
SBR	100	
Reinforced SBR-*g*-VTES		100
Silica	variable	0
Zinc oxide	3	3
Stearic acid	1	1
Sulfur	2.2	2.2
CBS	1.5	1.5
DPG	2	2

spectra was obtained on Bruker AC 250 MHz NMR, and grafted SBR was swollen with $CDCl_3$.[25] The corresponding vulcanization characteristics were studied using a Moving Die Rhometer (JC-2000E) at 160°C according to ASTM D 2084-95. Tensile strength and tear strength were measured using Electron Omnipotence Experiment Machine SANS-CMT 5105 (Shenzhen New Sansi, China) according to standard ASTM D 3185-1999 and ASTM D-624 using angle test pieces, respectively. The fracture surfaces of the samples were observed by JSM6700 scanning electron microscopy (SEM) on gold-coated surfaces, the reinforced raw rubber were fractured under −78°C. Dynamic mechanical analysis was performed using DMA/SDTA861e (Mettler-Toledo, Switzerland) in the tension mode, at a heating rate of 5°C/min from −70°C to 115°C at 1 Hz.

RESULTS AND DISCUSSION

Characterization of SBR-*g*-VTES

Figure 1(a) presents the ATR-FTIR spectra of SBR and SBR-*g*-VTES. It shows an intense peak at 2931 cm^{-1}, 1451 cm^{-1}, and 645 cm^{-1}, which is due to aliphatic C—H stretch, —CH_2 scissoring and C=C stretching band, respectively. The appearance of two shoulder peaks in SBR-*g*-VTES indicate that the presence of Si—O—Si and Si—O—C in the range 1080 cm^{-1} and 1140 cm^{-1}. Sánchez[26] has also found absorption band at 1080 cm^{-1} corresponding to Si—O—Si.

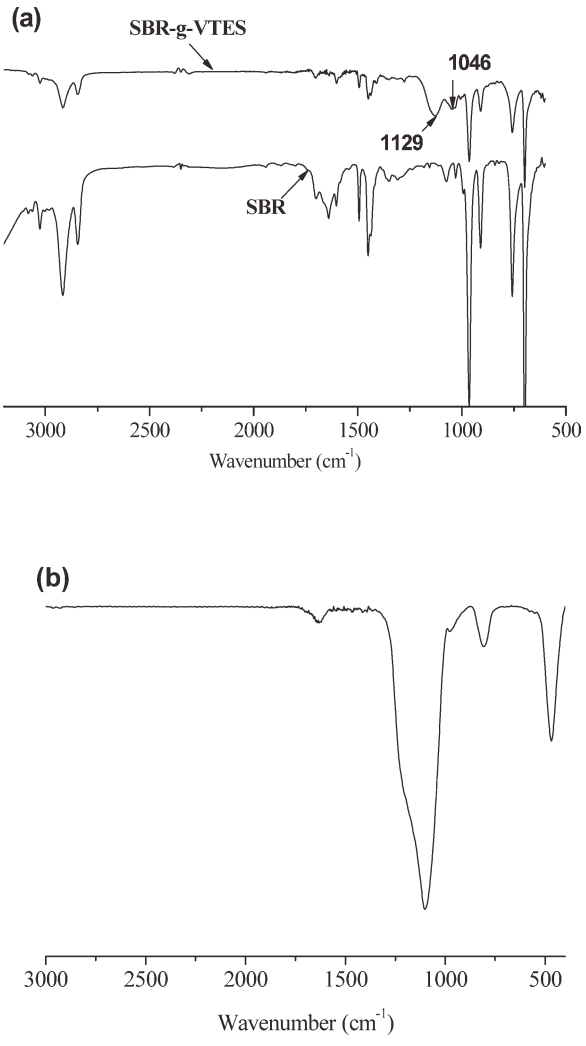

Figure 1. ATR-FTIR of SBR and SBR-*g*-VTES (a), FTIR of ashes of SBR-*g*-VTES (b).

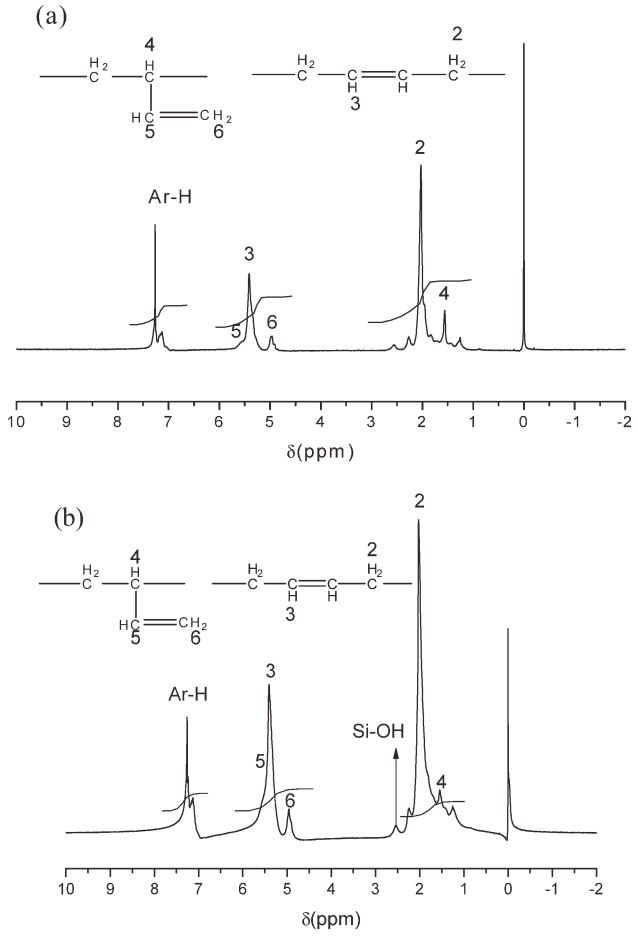

Figure 2. ^{1}H-NMR spectra of SBR (a) and SBR-*g*-VTES (b).

Figure 1(b) also shows the FTIR spectrum for the ash of SBR-*g*-VTES after burning under 700°C, and the appearance of the shoulder peak is ascribed to the presence of Si—O—Si in the range 1095 cm^{-1}(due to the SBR-*g*-VTES containing Si element). It can further prove that VTES has been grafted onto SBR successfully.

^{1}H-NMR was performed to confirm that VTES has been grafted onto the backbones of SBR. The corresponding results are shown in Figure 2.

Comparing with the ^{1}H-NMR spectra of ungrafted SBR, a new peak at 2.2–2.3ppm in SBR-*g*-VTES can be assigned to the Si—OH. At the same time, in Figure 2(a), the integrated areas of all the allylic hydrogen and double bond hydrogen are 58.86% and 27.25%, respectively. However, in Figure 2(b), the integrated areas of all the allylic hydrogen and double bond hydrogen are 58.23% and 25.39%, respectively. The decrease of double bond hydrogen indicates that the VTES has been successfully grafted onto the SBR, and the graft polymerization may occur on the double bond of the butadiene.

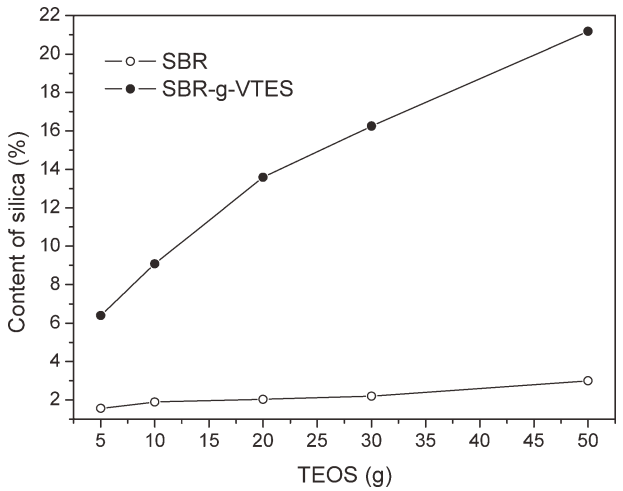

Figure 3. Amount of TEOS effecting on content of silica in SBR-*g*-VTES and SBR.

Content of Silica in Rubber and Utilized Efficiency of TEOS for Sol–Gel Process

The amount of TEOS added to SBR latex of 200 g in this study is designed from 5 to 50 g in order to investigate the content of silica and utilized efficiency of TEOS. The preparation conditions are shown in Table I. SBR and SBR-*g*-VTES latexes are easily mixed with TEOS without phase separation and flocculation.

Figure 3 shows the amount of TEOS effecting on the content of silica in SBR and SBR-*g*-VTES. The contents of silica in SBR and SBR-*g*-VTES increased with increasing amount of TEOS. It is attributed that the content of silica is almost controlled by amount of TEOS[27]. However, the content of silica in SBR-*g*-VTES is higher than that of SBR, and the difference becomes much larger with the increasing amount of TEOS. It is due to that lot of silica particles separated out individually, when the TEOS reinforced SBR latex reaction products are flocculated by flocculating agents. On the contrary, the alkoxysilyl (—$Si(OC_2H_5)_3$) groups in the SBR-*g*-VTES latex undergo the same hydrolysis and condensation reaction as the TEOS. When the TEOS are converted to silica particles, condensation reactions between SBR-*g*-VTES and silica particles can take place, and chemical bonding between rubber and silica particles is also formed. Meanwhile, the SBR-*g*-VTES latex can mix with TEOS more easily than that of SBR latex, and it can prevent the TEOS hydrolyzing in water continuous phase. As a result, more silica particles formed by TEOS will insert into the SBR-*g*-VTES networks. It is also believed that the polarity of the SBR-*g*-VTES causes strong effects on the content and distribution of silica in SBR matrix.

In the simplified manner, the tentative schematic grafted of SBR by VTES and subsequent hydrolysis and condensation reactions of TEOS to form silica particles reinforced SBR networks is presented in Figure 4. It can be concluded that the in situ silica particles are located in the SBR-*g*-VTES matrix or chemically bound with the SBR-*g*-VTES. Hashim[9] found similar results in the reinforcement of natural rubber. As a result, a higher utilized efficiency of TEOS and bound rubber will be observed in the SBR-*g*-VTES than that of SBR.

Figure 5 gives the relationships of TEOS with its utilized efficiency and bound rubber in SBR-*g*-VTES and ungrafted SBR.

It can be seen that the utilized efficiency of TEOS and bound rubber for SBR-*g*-VTES is higher than that of ungrafted SBR. The results are according with our consideration on chemical bonding formed between silica and rubber molecules (shown in Figure 4). Meanwhile, the utilized efficiency of TEOS of the both compounds is decreased with the increasing amount of TEOS. It is ascribed to that large silica particles are formed and separated from the matrix phase of the rubber with higher addition of TEOS. Yoshikai[4] reported that the silica particle size was affected by the amount of TEOS in silica reinforcement of SBR by sol–gel method.

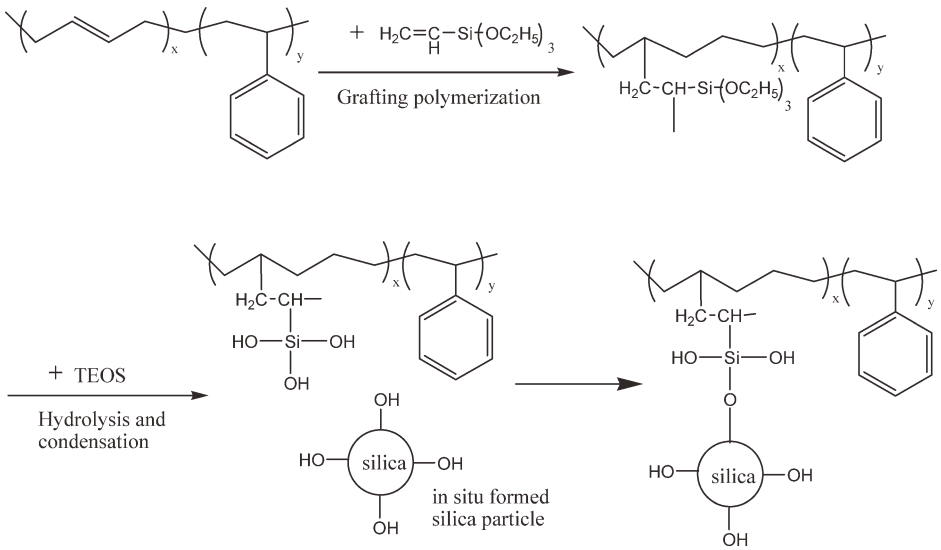

Figure 4. Grafting of SBR with VTES and subsequent hydrolysis and condensation reactions of TEOS to form silica particle reinforced SBR network.

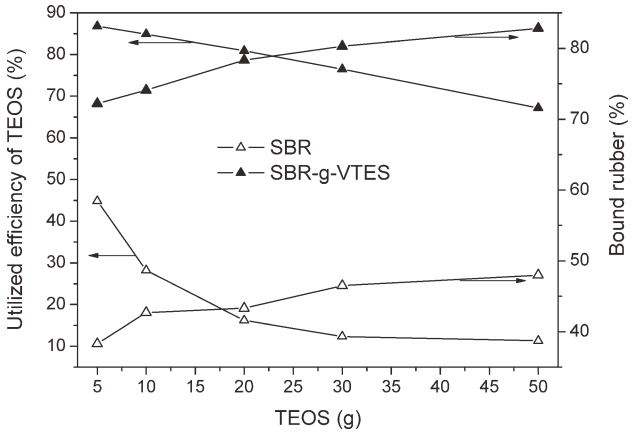

Figure 5. Amount of TEOS effecting on utilized efficiency of TEOS.

Curing Characteristics of *In Situ* Reinforced SBR-*g*-VTES and Silica-Reinforced SBR

The curing characteristics and mechanical properties of the vulcanized *in situ* reinforced SBR-*g*-VTES are investigated and compared with that of the SBR reinforced by equal amount of silica.

Torque of the Compounds. As the state of curing, delta torque reflects the crosslink density in the samples.[26] And the content of silica effecting on delta torques (maximum torque-minimum torque) of SBR, silica-reinforced SBR and *in situ* reinforced SBR-*g*-VTES are shown in Figure 6. It shows that all the delta torques of all compounds increased with the increasing content of silica. It is attributed that the incorporation of silica particles enhances the crosslink density of the rubber matrix.[27]

Meanwhile, the delta torque of *in situ* reinforced SBR-*g*-VTES is higher than that of silica-reinforced SBR and the difference becomes much larger with the increasing content of silica. It is due to that the formation of chemical bonds between the silica (formed by TEOS) and the ($Si(OC_2H_5)_3$) groups in SBR-*g*-VTES as shown in Figure 4.

Curing Time. Figure 7 shows the content of silica effecting on optimum curing time (t_{90}) of *in situ* reinforced SBR-*g*-VTES and silica-reinforced SBR.

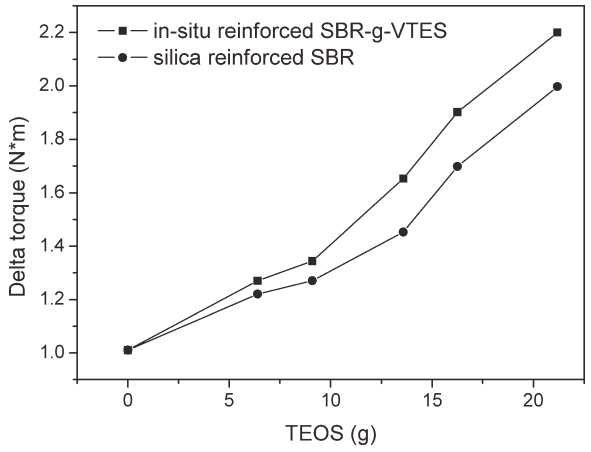

Figure 6. Content of silica effecting on delta torque of *in situ* reinforced SBR-*g*-VTES and silica-reinforced SBR.

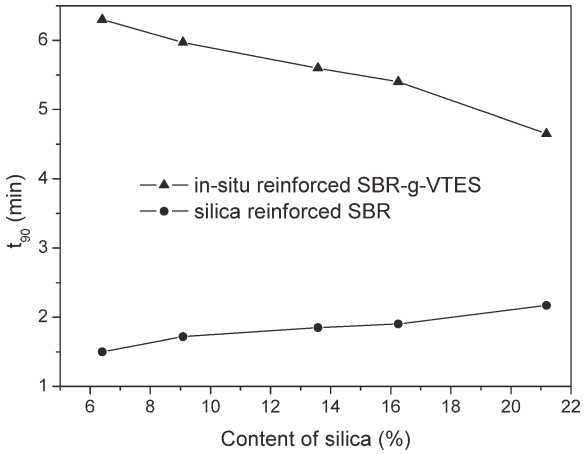

Figure 7. Content of silica effecting on curing time of *in situ* reinforced SBR-*g*-VTES and silica-reinforced SBR.

The t_{90} of *in situ* reinforced SBR-*g*-VTES decreased with the increasing content of silica. It can be explained that the rubber chains are occluded and fixed on the surface of the silica, in favor of accelerating the reaction rate. And the similar results of the reinforcing elastomers with mesoporous silica were found by León.[28] The t_{90} of silica-reinforced SBR is also increased with increasing content of silica, it is due to that the silica can absorb curing agents and block the movement of rubber chains.

Meanwhile, the t_{90} of reinforced SBR-*g*-VTES is longer than that of silica-reinforced SBR and the difference becomes smaller with the increasing content of TEOS. This is due to the lower concentration of double bonds in SBR-*g*-VTES.

Mechanical Properties

Stress–Strain Curves. Stress–strain curves of silica-reinforced SBR and *in situ* reinforced SBR-*g*-VTES with different contents of silica are shown in Figure 8.

It can be seen that the tensile modulus, elongation at break, and tensile strength of *in situ* reinforced SBR-*g*-VTES and silica-reinforced SBR both increased with the increasing content of

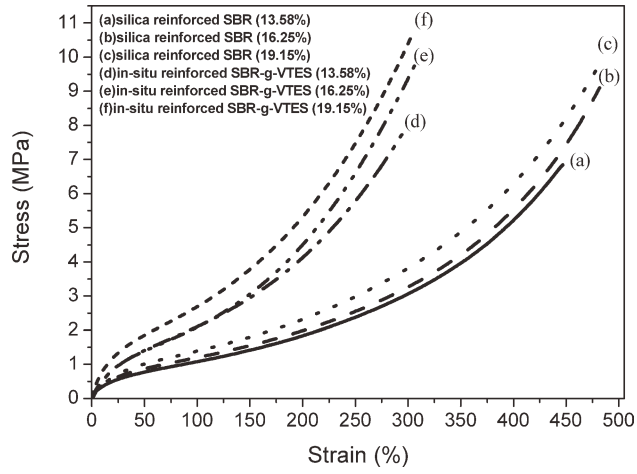

Figure 8. Stress–strain curves of silica-reinforced SBR and *in situ* reinforced SBR-*g*-VTES with different content of silica.

Applied Polymer SCIENCE

Table III. Content of Silica Effecting on the Tensile Strength and Tear Strength of *In Situ* Reinforced SBR-*g*-VTES and Silica-Reinforced SBR

Content of silica (mass%)	Tensile strength (MPa)		Tear strength (kN/m)	
	In situ method	Silica-reinforced	*In situ* method	Silica-reinforced
0	2.1	2.1	15.45	15.45
6.4	4.53	4.26	25.15	24.46
9.09	5.12	4.89	27.66	26.68
13.58	7.92	6.84	29.17	28.85
16.25	9.65	9.18	34.95	31.37
21.18	10.7	9.98	37.90	32.13

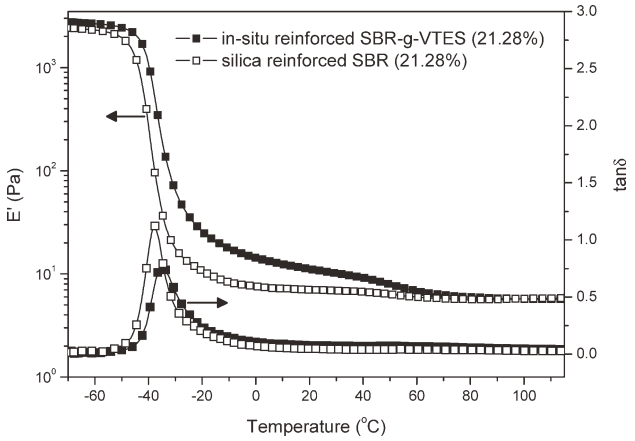

Figure 9. Temperature dependence of E' and tan δ of the *in situ* reinforced SBR-*g*-VTES and silica-reinforced SBR.

silica. Comparative analysis indicates that the *in situ* reinforced SBR-*g*-VTES has higher tensile modulus and tensile strength than that of silica-reinforced SBR. It is due to the presence of strong silica-rubber matrix interaction in *in situ* reinforced SBR-*g*-VTES, and it causes a large amount of restriction to the movement of silica particles against applied deformation. However, the elongation at break of *in-situ* reinforced SBR-*g*-VTES is lower than that of silica-reinforced SBR. It is due to higher cross-linking density in this case compared with silica-reinforced SBR, which makes it less elastic.

The content of silica effecting on the tensile strength and tear strength of *in situ* reinforced SBR-*g*-VTES and silica-reinforced SBR are shown in Table III. It can be seen that tensile strength and tear strength of *in situ* reinforced SBR-*g*-VTES and silica-reinforced SBR are increased with the increasing content of silica. It is due to that silica can absorb the pull powers and realize the desperation of pull power, therefore increase the properties of rubber. The higher tensile strength and tear strength are also observed for *in situ* reinforced SBR-*g*-VTES. It

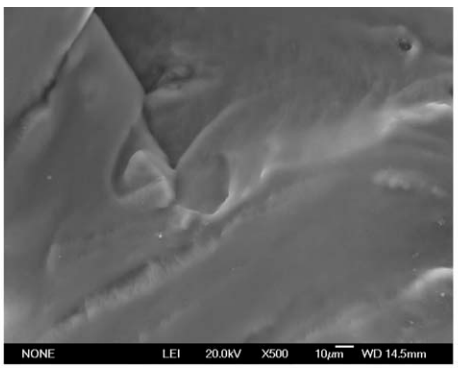

(a)

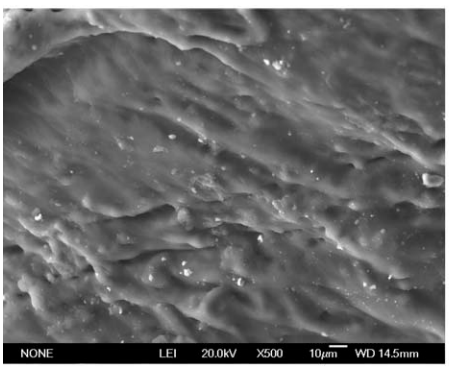

(b)

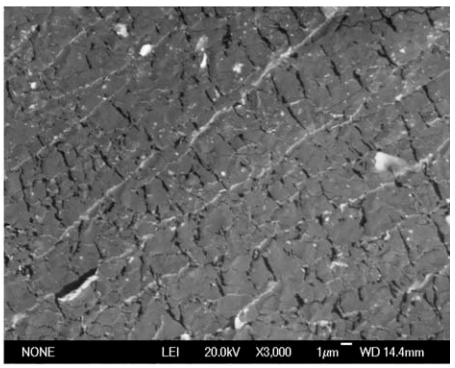

(c)

Figure 10. SEM pictures of cryogenically fractured surfaces: (a) SBR; (b) silica-reinforced; (c) *in situ* reinforced SBR-*g*-VTES.

is due to the chemically interaction between silica and SBR in *in situ* reinforced SBR-*g*-VTES.

Dynamic Mechanical Properties. Temperature dependence on the dynamic mechanical properties of cured *in situ* reinforced SBR-*g*-VTES and silica-reinforced SBR are shown in Figure 9. It is observed that the storage modulus of *in situ* reinforced SBR-*g*-VTES is higher than that of silica-reinforced a reinforced SBR, especially at the rubbery zone ($T > T_g$). It is attributed to that the interaction of interparticles formed by TEOS is higher than that of the directly added silica by mechanical mixing.

The glass transition temperature (T_g) of the samples is estimated by means of the maximum value in the loss factor curves. It can be seen that, the T_g of silica-reinforced SBR and *in situ* reinforced SBR-*g*-VTES is $-38°C$ and $-34.6°C$, respectively. The small shift to higher temperatures can be associated with the imposed restrictions due to the interaction between the silica and the SBR chains. Meanwhile, the loss factor values of *in situ* reinforced SBR-*g*-VTES at $-20 \sim 0°C$ are slightly higher than that of silica-reinforced SBR.

Dispersed Silica in Silica-Reinforced SBR and *In Situ* Reinforced SBR-*g*-VTES

Figure 10 shows the SEM photographs of raw SBR (a), silica-reinforced SBR contained 16.25% silica (b), and TEOS reinforced SBR-*g*-VTES contained 16.25% silica (c), respectively.

It can be seen that, the rough surface is observed in silica-reinforced SBR as shown in Figure 10(b). It reveals low adhesion between SBR and silica. However, as seen from *in situ* reinforced SBR-*g*-VTES by TEOS as shown in Figure 10(c), the typical brittle fracture characteristics "completely smooth surface" is observed. It is attributed that the interaction between SBR and silica are enhanced in SBR-*g*-VTES.

CONCLUSIONS

The grafting polymerization pf VTES onto SBR was successfully carried out using KPS as initiator in SBR latex. Then the TEOS reinforced SBR-*g*-VTES were prepared by *in situ* sol–gel method in SBR-*g*-VTES latex. The grafting VTES onto SBR was ascertained from ATR-FTIR and ^{1}H-NMR. Compared with the content of silica in ungrafted SBR, the content of silica in SBR-*g*-VTES increases 7.06 times. The crosslink density, tensile strength, and tear strength of the SBR-*g*-VTES increased with the increasing concentration of TEOS. Compared with mechanical mixing, the improvement in mechanical properties and dynamic mechanical properties may be explained by the increased chemical interaction between SBR-*g*-VTES and silica.

ACKNOWLEDGMENTS

This work was financially supported by National Basic Research Program of China (Grant No. 2010CB635111 and the Basic Research of Northwestern Polytechnical University (Grant No. G9KY1020).

REFERENCES

1. Shigeyuki, O.; Yasutaro, K.; Junich, S.; Masayoshi, I. *Polym. Int.* **1999,** *48*, 1035.
2. Ramier, J.; Gauthier, C.; Chazeau, L.; Stelandre, L. G. *J. Polym. Sci. Part B: Polym. Phys.* **2007,** *45*, 286.
3. Wolff, S.; Wang, M. J.; Tan, E. H. *Kautsch Gummi Kunst* **1994,** *47*, 780.
4. Schoon, T. G. F.; Adler, K. *Kautsch Gummi Kunst* **1966,** *19*, 414.
5. Roychoudhury, A. De; Roychoudhury, P. P.; Vidal, N. *J. Appl. Polym. Sci.* **1995,** *55*, 9.
6. Verughese, S.; Tripathy, D. K. *J. Appl. Polym. Sci.* **1992,** *44*, 1847.
7. Ikeda, Y.; Kohjiya, S. *Polymer* **1997,** *38*, 4417.
8. Bokobzaa, L.; Chauvinb, J. P. *Polymer* **2005,** *46*, 4144.
9. Hashim, A. S.; Kohjiya, S.; Ikeda, Y. *Polym. Int.* **1995,** *38*, 111.
10. Ikeda, Y.; Kameda, Y. *J. Sol-Gel. Sci. Technol.* **2004,** *31*, 137.
11. Murakami, K.; Iio, S.; Ikeda, Y., et al. *J. Mater. Sci.* **2003,** *38*, 1447.
12. De, D.; Das, A.; Kumar, P., et al. *J. Appl. Polym. Sci.* **2006,** *99*, 957.
13. Duan, X.; Wu, S.; Zhong, R., et al. *China Synthetic Rubber Industry* **2001,** *24*, 234.
14. de LucaM, A.; Machado, T. E. *J. Appl. Polym. Sci.* **2004,** *92*, 798.
15. Bandyopadhyay, A.; de Sarkar, M.; Bhowmick, A. K. *J. Mater. Sci.* **2005,** *40*, 53.
16. Massimo, M.; Maurizio, F. *J. Appl. Polym. Sci.* **2011,** *119*, 3422.
17. Massimo, M.; Fabio, B.; Riccardo, De S.; Rosa, T. *Polym. Int.* **2009,** *58*, 880.
18. Joanna, P.; Magdalena, G.; Marian, Z.; Lidia, O.; Gisèle, B.; Olivier, G. *Eur. Polym. J.* **2009,** *45*, 3317.
19. Kazumasa, Y.; Tetsuro, O.; Mutsuhisa, F. *J. Appl. Polym. Sci.* **2002,** *85*, 2053.
20. Alagar, M.; Abdul Majeed, S. M.; Nagendiran, S. *Polym. Adv. Technol.* **2005,** *16*, 582.
21. Kawada, T.; Hikita, M.; Makino, K. *Jpn Pat JP 6* **1998,** *325* 610.
22. Natchamon, W.; Sirilux, P.; Pattarapan, P. *J. Sol-Gel Sci. Technol.* **2011,** *58*, 407.
23. Yin, C.; Zhang, Q.; Yin, D. *J. Appl. Polym. Sci.* **2011,** *119*, 2808.
24. Yin, C.; Zhang, Q.; Yin, D.; Zhao, X.; Zheng, J. *Polym. Mater. Sci. Eng.* **2011,** *27*, 160.
25. Seo, B. D.; Park, D. J.; Ha, C. S.; Cho, W. J. *J. Appl. Polym. Sci.* **1995,** *8*, 1255.
26. Sung-Seen, C.; Byung-Ho, P.; Hanjong, S. *Polym. Adv. Technol.* **2004,** *15*, 122.
27. María, D.; Romero-Sánchez, M.; Mercedes, P.-B.; José Miguel, M.-M. *Int. J. Adhes. Adhes.* **2001,** *21*, 325.
28. León, D. P.; Luis, F. G.; Brtty, L. L.; Michael, H. *Macromol. Symp.* **2006, 245.**